

# Lawrence Berkeley National Laboratory

## LBL Publications

### Title

Note: Setup for chemical atmospheric control during in situ grazing incidence X-ray scattering of printed thin films

### Permalink

<https://escholarship.org/uc/item/1kv511q3>

### Journal

Review of Scientific Instruments, 88(6)

### ISSN

0034-6748

### Authors

Pröllner, Stephan

González, Daniel Moseguí

Zhu, Chenhui

et al.

### Publication Date

2017-06-01

### DOI

10.1063/1.4984130

Peer reviewed

## Note: Setup for chemical atmospheric control during in situ grazing incidence X-ray scattering of printed thin films

Stephan Pröller, Daniel Moseguí González, Chenhui Zhu, Eric Schaible, Cheng Wang, Peter Müller-Buschbaum, Alexander Hexemer, and Eva M. Herzig

Citation: [Review of Scientific Instruments](#) **88**, 066101 (2017); doi: 10.1063/1.4984130

View online: <http://dx.doi.org/10.1063/1.4984130>

View Table of Contents: <http://aip.scitation.org/toc/rsi/88/6>

Published by the [American Institute of Physics](#)

---

### Articles you may be interested in

[Imaging at an x-ray absorption edge using free electron laser pulses for interface dynamics in high energy density systems](#)

[Review of Scientific Instruments](#) **88**, 053501 (2017); 10.1063/1.4982166

[A physics-based solver to optimize the illumination of cylindrical targets in spherically distributed high power laser systems](#)

[Review of Scientific Instruments](#) **88**, 053503 (2017); 10.1063/1.4979932

[Generation and application of LET calibration curve for neutron dosimetry using CR-39 detector and microwave induced chemical etching](#)

[Review of Scientific Instruments](#) **88**, 063301 (2017); 10.1063/1.4984621

[Coarse spectral characterization of warm x-rays at the Z facility using a filtered thermoluminescent dosimeter array](#)

[Review of Scientific Instruments](#) **88**, 043501 (2017); 10.1063/1.4979626

[Analyzing X-ray tomographies of granular packings](#)

[Review of Scientific Instruments](#) **88**, 051809 (2017); 10.1063/1.4983051

[A compact two-way power divider based on five-port structure](#)

[Review of Scientific Instruments](#) **88**, 064701 (2017); 10.1063/1.4984294

---



**JANIS**

**Janis Dilution Refrigerators & Helium-3 Cryostats  
for Sub-Kelvin SPM**

**Click here for more info [www.janis.com/UHV-ULT-SPM.aspx](http://www.janis.com/UHV-ULT-SPM.aspx)**

## Note: Setup for chemical atmospheric control during *in situ* grazing incidence X-ray scattering of printed thin films

Stephan Pröller,<sup>1</sup> Daniel Moseguí González,<sup>2</sup> Chenhui Zhu,<sup>3</sup> Eric Schaible,<sup>3</sup> Cheng Wang,<sup>3</sup> Peter Müller-Buschbaum,<sup>2</sup> Alexander Hexemer,<sup>3</sup> and Eva M. Herzig<sup>1,4,a)</sup>

<sup>1</sup>Munich School of Engineering, Herzig Group, Technische Universität München, Lichtenbergstr. 4a, 85748 Garching, Germany

<sup>2</sup>Physik Department, Lehrstuhl für Funktionelle Materialien, Technische Universität München, James-Frank Str. 1, 85748 Garching, Germany

<sup>3</sup>Advanced Light Source, Lawrence Berkeley National Laboratory, 1 Cyclotron Rd., Berkeley, California 94720, USA

<sup>4</sup>Experimentalphysik II, Universität Bayreuth, Universitätsstr. 30, 95440 Bayreuth, Germany

(Received 21 February 2017; accepted 10 May 2017; published online 1 June 2017)

In order to tailor the assembling of polymers and organic molecules, a deeper understanding of the kinetics involved in thin film production is necessary. While post-production characterization only provides insight on the final film structure, more sophisticated experimental setups are needed to probe the structure formation processes *in situ* during deposition. The drying kinetics of a deposited organic thin film strongly influences the assembling process on the nanometer scale. This work presents an experimental setup that enables fine control of the atmosphere composition surrounding the sample during slot die coating, while simultaneously probing the film formation kinetics using *in situ* grazing incidence X-ray scattering and spectroscopy. *Published by AIP Publishing.* [<http://dx.doi.org/10.1063/1.4984130>]

The increasing interest in organic electronics (OEs), especially in organic light emitting diodes (OLEDs), organic solar cells (OSCs), and organic field effect transistors (OFETs) demands production possibilities on large scale. As organic semiconductors can be processed out of solution, up-scalable printing techniques like slot die coating or spraying are methods of choice for thin film deposition.<sup>1,2</sup> For an OSC, the device architecture and the resulting inner nano-morphology are important for the device performance.<sup>3,4</sup> Several attempts aim to manipulate the inner morphology either during processing of the active layer or thereafter. The most prominent ones are thermal annealing, solvent additives, or solvent annealing, where especially the latter one is a promising approach.<sup>5–7</sup> A 3D reconstruction of the final inner structure can, for example, be obtained using ptychographic X-ray imaging.<sup>8</sup> To gain control over the final structure, current interest has moved on to investigate the kinetics during morphology formation using grazing incidence small and wide angle X-ray scattering (GISAXS/GIWAXS). Recently, the first attempt of a slot die coater adaptable to synchrotron beamlines was introduced and mechanisms of structure formation of printed films were shown.<sup>9,10</sup> To understand the self-assembly processes in thin organic films, advanced setups for *in situ* characterization implemented into a synchrotron instrument are required, while having control over various parameters.<sup>11–13</sup> In this work, we design and fabricate a modular chamber for the slot die coater that was previously introduced.<sup>9,10</sup> This chamber enables full control during the printing of thin films while allowing for *in situ* characterization of the film formation. It is capable of

offering and keeping a defined flow of different wet gases containing organic solvents with customized partial pressures, featuring the whole range from dry to solvent-saturated gas, which allows for annealing during device processing. Further control parameters can be used, for example, an external electric field or a defined sample stage temperature. During processing, the morphological development can be tracked *in situ* with GISAXS, GIWAXS, and optical spectroscopy. To demonstrate the functionality of the setup, it is implemented into a synchrotron instrument and the drying of a printed active layer for OSCs is probed with GISAXS. Additionally, we are able to track the changes in the absorption behavior during decelerated solidification.

The main part of the presented setup is a chamber, in which the sample printing takes place. A diagram of the complete printer setup (printing unit and environmental chamber) is depicted in Fig. 1(a), see the [supplementary material](#) for further images. The presented chamber is generally made of aluminum plates for good chemical resistance against organic solvents at low weight. The inner volume is kept small to keep the time scale of atmosphere control as short as possible. The outer dimensions are around (130 × 300) mm<sup>2</sup> with a height of 80 mm except at the outlet window with a height of 100 mm in order to extend the scattering exit angle range for GIWAXS. For weight reduction, all sides exhibit milled pockets but still guarantee a high stability and the possibility to weld the chamber sides together for high gas tightness. It is mounted above the horizontal motor by spacers carrying the weight and fixing the position of the chamber. The motor is kept outside the chamber to separate the electrical components from the solvent atmosphere and, concurrently, minimize the volume of the chamber. The lateral movement of the motor stage is then transferred into the static chamber via rails fixed

<sup>a)</sup> Author to whom correspondence should be addressed: [eva.herzig@ph.tum.de](mailto:eva.herzig@ph.tum.de).

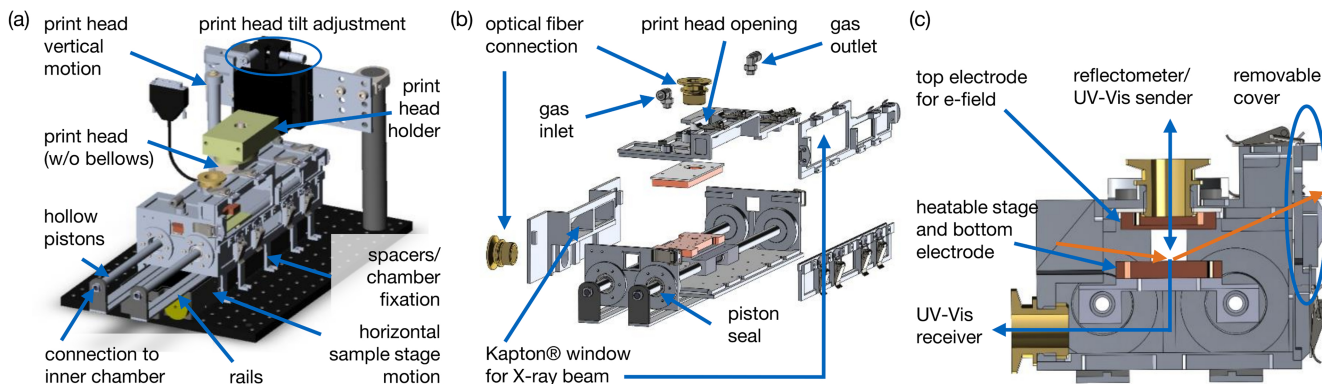


FIG. 1. (a) Isometric view of the fully assembled printer setup including the printing unit and the environmental control chamber. (b) Exploded isometric view of the atmosphere chamber with most important functional parts. (c) Sectional front view on the sample stage and the connection possibilities for optical fibers for *in situ* reflectometry or UV-Vis measurements. The orange arrows schematically depict the X-ray path relative to the chamber.

on the motor stage and parallel mounted, sealed (Zurcon® Z20, Trelleborg Sealing Solutions) hollow pistons. Inside the chamber, a holder is fixed on these pistons, on which there is an electrically heatable (up to 150 °C) sample stage that moves with the pistons inside the chamber. High performance resistors are mounted on the bottom of the copper stage and are connected via electrical plugs that are mounted into the end of the hollow pistons and sealed by casting epoxy. The stage holder is made of polyether ether ketone (PEEK), which exhibits a low thermal expansion along with a high solvent resistivity. The copper stage also works as the bottom electrode, which together with a copper top electrode allows for an electric field during printing. The maximum length of a coated film is 150 mm, which is sufficient for following the film solidification process. The heatable print head (Jema Technologies LLC) is positioned inside the chamber through an opening in its ceiling. To ensure the tightness, bellows (side) and a print head holder (top) are used. The holder is made of PEEK for low heat conduction to the mount and sealed using area seals. This allows to vertically move the print head and thereby adjusting an accurate print head-to-sample distance (gap clearance), while remaining an atmosphere tight environment inside the chamber. A removable cover that enables the exchange of samples is sealed with a surface seal and fixed with snap locks during operation. The individual parts and their positions are depicted in the exploded, isometric view of Fig. 1(b) as well as in the sectional front view in Fig. 1(c).

To produce the desired atmosphere two gas supplies, dry and saturated, respectively, are mixed at a controlled ratio. Solvent-saturated gas is obtained using a washing bottle. Each path's flow is regulated separately using mass flow controllers (red-y smart controller GSC, Vögtlin Instruments AG). Afterwards, both supplies are merged to produce a gas mixture in a ratio according to the set flow rates and directed into the chamber via a nozzle purchased from Lechler GmbH at the gas inlet. This nozzle provides a defined gas flow above the sample. To probe the sample with X-rays, 25.4  $\mu\text{m}$  thick Kapton® foils from DuPont™ are fixed on either side of the chamber. The setup is designed to observe the main characteristic crystalline peaks of most semiconducting polymers of interest (maximum achievable  $q_z = 18 \text{ nm}^{-1}$ ,  $q_{xy} = 25 \text{ nm}^{-1}$  for 10 keV). The remaining windows are covered with glass

for illumination and acquisition of a video signal to be able to control the process remotely, which is necessary for *in situ* X-ray probing. Further features are the KF flanges mounted on the top and side of the chamber to connect optical fibers to an UV-Vis sender and receiver or a reflectometer, respectively. Hence, either the film thickness or the absorption properties of the printed film can be probed while drying. The sectional front view in Fig. 1(c) identifies the paths of optical and X-ray characterization. The top fiber is lead through a copper plate which also works as the top electrode for the electrical field. A hole in the copper sample stage and its holder allow the UV-Vis signal to pass the stage.

Two experiments on the model system poly(3-hexylthiophene):[6,6]-phenyl-C61 butyric acid methyl ester (P3HT:PCBM) in chlorobenzene (20 mg/ml, 1:1 ratio), widely used for OSCs, are carried out to demonstrate the versatility of the environmental chamber. Therefore, as a first experiment, it is implemented into beamline 7.3.3 of the Advanced Light Source (ALS) at Lawrence Berkeley National Laboratory.<sup>14</sup> The P3HT:PCBM blend is printed on a silicon substrate using different gas streams flowing above the freshly coated film. The printing parameters are set to a pump rate of 250  $\mu\text{l}/\text{min}$ , a printing speed of 10 mm/s, and a gap clearance of around 300  $\mu\text{m}$ , resulting in a final film thickness of around 150 nm. Time-resolved GISAXS is performed *in situ* to track the structure formation while drying with an incident angle of 0.35°, similar to previous studies on this material,<sup>4,10</sup> and a sample-to-detector distance of 1.8 m at 10 keV. Figs. 2(a) and 2(b) depict vertical line cuts of the recorded 2D-GISAXS data versus time for a sample printed under a flow of dry helium gas and chlorobenzene saturated helium gas. The data show a clear difference in the structure formation time for the two different experimental conditions. Drying under a dry gas flow shows a rapidly increasing scattering signal, whereas the sample coated under a saturated flow shows initially a decelerated process, which then rapidly increases at a later stage. The slower drying is expected to influence the structure formation in a positive manner in terms of solar cell efficiency.<sup>7,10</sup>

The second demonstration experiment shows the suitability of the implemented optical fibers to record absorption spectra of the printed films during thin film solidification

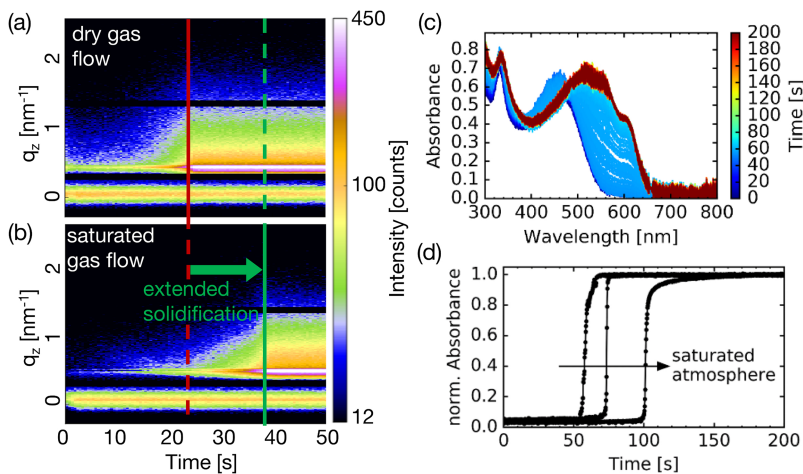


FIG. 2. Left: Mappings of  $q_z$  intensity profiles versus time obtained from cuts next to the beam-stop for every single 2D scattering pattern obtained with DPDAK.<sup>15</sup> The structure formation in the vertical direction can be followed. P3HT:PCBM sample printed under a constant flow of (a) dry helium and (b) chlorobenzene saturated gas showing a much slower structure formation process. The intensity and time scale refer to both datasets. (c) UV-Vis spectra recorded under a dry gas flow showing the aggregation of the P3HT:PCBM blend film evolving with a time resolution of 200 ms directly after the printing process. (d) Tracking of the absorption shoulder of the P3HT crystal at  $\lambda = 605$  nm for differently chlorobenzene-wetted atmospheres as indicated with the arrow.

exemplified by printing a P3HT:PCBM film on a glass substrate in nitrogen atmosphere. The recorded UV-Vis spectra during printing are shown in Fig. 2(c). With a time resolution of 200 ms, the crystallization process can clearly be followed. After the initial evaporation of the solvent, the polymer crystallizes within 10-20 s as seen in the formation of well-established shoulders in the UV-Vis spectra at around 605 nm. Using a chlorobenzene-saturated nitrogen gas stream while printing, the onset of the crystallization shoulder is delayed for approximately 20 s [Fig. 2(d)]. If the gas flow is switched on 10 min prior to printing, the solvent partial pressure inside the chamber is able to increase, which yields a delay of even up to nearly double the time compared to the film printed under a dry flow. Thus, the data confirm the proper functioning of the atmospheric chamber allowing for customized conditions of film printing along with comprehensive morphological and spectroscopic system characterizations.

In this work, we have designed and built an atmospheric chamber for a slot die coater which can be implemented into a synchrotron beamline for *in situ* measurements of the structure formation. Using the presented setup, it is possible to transfer the controlled printing of thin films into a synchrotron beamline offering a detailed analysis of the fundamentals of structure formation while controlling the environment to approach optimized film production conditions. The setup offers the possibility to simultaneously track either the film thickness or the absorption properties with a reflectometer and UV-Vis, respectively. The structure formation time of a model P3HT:PCBM system is reduced by controlling the vapor environment during printing as seen with *in situ* GISAXS and UV-Vis absorption measurements. Using the presented setup, the self-assembly process in thin films is controlled by tuning several macroscopic processing parameters (vapor environment, flow rate of gases, temperature, external electric field, etc.) which enable the production of functional films with enhanced properties.

See [supplementary material](#) for further large scale views of the chamber.

We acknowledge the financial support by the Bavarian State Ministry of Education, Science and the Arts via

the project “Energy Valley Bavaria,” from BaCaTec and the Dr.-Ing. Leonhard-Lorenz-Stiftung. We thank Marc Schönberger and Erik Faber for support and manufacturing the setup. P.M.-B. and D.M.G. acknowledge financial support by TUM.solar via “Solar technologies go Hybrid” (SolTec), the GreenTech Initiative (Interface Science for Photovoltaics - ISPV) of the EuroTech Universities, and the Nanosystems Initiative Munich (NIM). Beamline 7.3.3 of the Advanced Light Source is supported by the Director of the Office of Science, Office of Basic Energy Sciences, of the U.S. Department of Energy under Contract No. DE-AC02-05CH11231.

- <sup>1</sup>R. R. Søndergaard, M. Hösel, and F. C. Krebs, *J. Polym. Sci., Part B: Polym. Phys.* **51**, 16 (2013).
- <sup>2</sup>P. Zhang, G. Santoro, S. Yu, S. K. Vayalil, S. Bommel, and S. V. Roth, *Langmuir* **32**, 4251 (2016).
- <sup>3</sup>M. A. Brady, G. M. Su, and M. L. Chabiny, *Soft Matter* **7**, 11065 (2011).
- <sup>4</sup>W. Wang, S. Pröller, M. A. Niedermeier, V. Körstgens, M. Philipp, B. Su, D. Moseguí González, S. Yu, S. V. Roth, and P. Müller-Buschbaum, *ACS Appl. Mater. Interfaces* **7**, 602 (2015).
- <sup>5</sup>A. M. Hiszpanski and Y.-L. Loo, *Energy Environ. Sci.* **7**, 592 (2014).
- <sup>6</sup>Y. Chen, C. Zhan, and J. Yao, *Chem.-Asian J.* **11**, 2620 (2016).
- <sup>7</sup>G. Li, Y. Yao, H. Yang, V. Shrotriya, G. Yang, and Y. Yang, *Adv. Funct. Mater.* **17**, 1636 (2007).
- <sup>8</sup>H. F. Dam, T. R. Andersen, E. B. L. Pedersen, K. T. S. Thydén, M. Helgesen, J. E. Carlé, P. S. Jørgensen, J. Reinhardt, R. R. Søndergaard, M. Jørgensen, E. Bundgaard, F. C. Krebs, and J. W. Andreasen, *Adv. Energy Mater.* **5**, 1400736 (2015).
- <sup>9</sup>F. Liu, S. Ferdous, E. Schaible, A. Hexemer, M. Church, X. Ding, C. Wang, and T. P. Russell, *Adv. Mater.* **27**, 886 (2015).
- <sup>10</sup>S. Pröller, F. Liu, C. Zhu, C. Wang, T. P. Russell, A. Hexemer, P. Müller-Buschbaum, and E. M. Herzig, *Adv. Energy Mater.* **6**, 1501580 (2016).
- <sup>11</sup>X. Gu, J. Reinspach, B. J. Worfolk, Y. Diao, Y. Zhou, H. Yan, K. Gu, S. Mannsfeld, M. F. Toney, and Z. Bao, *ACS Appl. Mater. Interfaces* **8**, 1687 (2016).
- <sup>12</sup>L. H. Rossander, N. K. Zawacka, H. F. Dam, F. C. Krebs, and J. W. Andreasen, *AIP Adv.* **4**, 87105 (2014).
- <sup>13</sup>M. Sanyal, B. Schmidt-Hansberg, M. F. G. Klein, A. Colsmann, C. Munuera, A. Vorobiev, U. Lemmer, W. Schabel, H. Dosch, and E. Barrena, *Adv. Energy Mater.* **1**, 363 (2011).
- <sup>14</sup>A. Hexemer, W. Bras, J. Glossinger, E. Schaible, E. Gann, R. Kirian, A. MacDowell, M. Church, B. Rude, and H. Padmore, *J. Phys.: Conf. Ser.* **247**, 12007 (2010).
- <sup>15</sup>G. Benecke, W. Wagermaier, C. Li, M. Schwartzkopf, G. Flucke, R. Hoerth, I. Zizak, M. Burghammer, E. Metwalli, P. Müller-Buschbaum, M. Trebbin, S. Förster, O. Paris, S. V. Roth, and P. Fratzl, *J. Appl. Crystallogr.* **47**, 1797 (2014).